versity of California, Santa Barbara (1977).
Matheron, E. R., and O. C. Sandall, "Gas Absorption Accompanied by a Second-order Chemical Reaction Modeled According to the Danckwerts Surface Renewal Theory," *AIChE*, **24**, 552 (1978).
Menez, G. D., and O. C. Sandall, "Gas Absorption Accompanied by First-Order Chemical Reaction in Turbulent Liquids," *Ind. Eng. Chem. Fund.*, **13**, 72 (1974).
Nijsing, R. A. T. O., R. H. Hendriks, and H. Kramers, "Absorption of CO_2 in Jets and Falling Films of Electrolyte Solutions, with and without Chemical Reaction," *Chem. Eng. Sci.*, **1**, 88 (1959).
Pearson, J. R. A., "Diffusion of One Substance into a Semi-Infinite Medium Containing Another with Second-Order Reaction," *Appl. Sci. Res. Sec.*, A, **11**, 321 (1963).
Perez, J. F., and O. C. Sandall, "Diffusivity Measurements for Gases in Power Law Non-Newtonian Liquids," *AIChE J.*, **19**, 1073 (1973).
Pinsent, B. R. W., L. Pearson, and F. J. W. Roughton, "The Kinetics of Combination of CO_2 with OH^-," *Trans. Far. Soc.*, **52**, 1512 (1956).

Manuscript received August 4, 1981; revision received March 31, and accepted April 19, 1982.

Unified Treatment of Structural Effects in Fluid-Solid Reactions

S. K. BHATIA and D. D. PERLMUTTER

**Department of Chemical Engineering
University of Pennsylvania
Philadelphia, PA 19104**

By considering reaction and diffusion through a product layer and concomitant movement of pore and reaction surfaces, a general rate equation is derived for fluid-solid reactions. Application to the random pore model extends the prior results (Bhatia and Perlmutter, 1980, 1981a) to account for nonlinear concentration gradients in the product layer, by assuming that the product is deposited as overlapping cylindrical annulae. For the Petersen (1957) model, new results are derived which account for product layer diffusion. A comparison of numerical conversion-time predictions from the grain model (Szekely et al., 1976), the Petersen model, and the random pore models suggests that they are more strongly affected by the representation of the reaction surface than by that of the pore surface. The model is applied to the data of Borgwardt (1970) on the SO_2-lime reaction, and the results are compared with a previous interpretation using a linear concentration gradient approximation.

SCOPE

For fluid-solid chemical reactions, a general rate equation is derived which treats the various existing models (Petersen, 1957; Szekely et al., 1976; Bhatia and Perlmutter, 1980, 1981a) in a single unified analytical framework involving the simultaneous motion of pore and reaction surfaces. The distinction among the different models is made in terms of only the several representations of these motion.

Prior representations of the motion of the pore surface have on occasion yielded inconsistent results. Thus, for example, expanding grain models (Georgakis et al., 1979) predict an ever-increasing pore surface area in spite of a decrease in pore volume. The random pore model developed by Bhatia and Perlmutter (1981a) considers the pore and reaction surface areas to be equal, an approximation which, of necessity, is less accurate at high conversions. The extension of the Petersen (1957) model by Calvelo and Cunningham (1970) accounts for product formation, but not for any product layer diffusional resistance or changes in pore surface area.

The influence of the motion of the pore and reaction surfaces on conversion behavior is analyzed and compared for the various structural models. The results are applied to the experimental data of Borgwardt (1970).

CONCLUSIONS AND SIGNIFICANCE

A generalized approach is presented to predict fluid-solid reaction behavior for a variety of structural assumptions on the solid. An important basis in the model, that each point on the growing or shrinking reaction surface moves at the same rate, is exact for a uniform pore or grain-size solid reactant.

A comparison of the grain model, the Petersen model, and the model developed here shows that the representation of the pore surface effects the predicted conversion behavior less severely than that of the reaction surface, unless the reaction is accompanied by a substantial increase in the volume of the solid phase, or when product layer diffusion is slow compared to reaction. When this is not the case, conversion time measurements under conditions of kinetic control should alone suffice to distinguish between the models.

Application of the model developed here to the experimental data of Borgwardt (1970) on the SO_2-lime reaction, yields an activation energy for product layer diffusion of 108 MJ/kmol, suggesting a solid-state process. Comparison of the estimated product layer diffusivities with those obtained using the previous thin layer model (Bhatia and Perlmutter, 1981b) shows that the latter calls for larger diffusivity because it predicts slower reaction rates. This difference is enhanced at elevated temperatures where higher levels of conversion are attained.

Current address of S. K. Bhatia: Department of Chemical Engineering, University of Florida, Gainesville, FL 32611.

INTRODUCTION

The assumption that reaction rate is proportional to surface area is common to several models that have been proposed to describe reaction between a fluid and a porous solid (Szekely et al., 1976). The individual results differ primarily in their respective methods of representing the structure of this internal surface and its variation with conversion. In the grain models (Barner and Mantell, 1968; Szekely and Evans, 1970; Calvelo and Smith, 1971), it is assumed that the solid is comprised of uniformly-sized grains of some idealized shape, spherical, cylindrical or cubical, each of which reacts in a shrinking core fashion. For spherical grains undergoing an irreversible first-order reaction:

$$aA(f) + bB(s) \rightarrow pP(f) + qQ(s) \tag{1}$$

Georgakis et al. (1979) have provided the result:

$$\frac{dX}{dt} = \frac{k_s S_0 C(1-X)^{2/3}}{(1-\epsilon_0)\left[1 + \frac{3\beta}{2}\left[(1-X)^{1/3} - \frac{(1-X)^{2/3}}{[1+(Z-1)X]^{1/3}}\right]\right]} \tag{2}$$

in which it is assumed that the fluid A diffuses through a spherical shell of product Q that surrounds an unreacted core of B in each grain, before reaction at the $B - Q$ interface. It has been noted by Bhatia and Perlmutter (1980) that such a model can only describe systems without a rate maximum, since it treats the reaction surface as monotonically shrinking. A changing grain-size approach has also been adopted by Ramachandran and Smith (1977a).

Among the earliest pore models, the one due to Petersen (1957) analyzed the complete gasification of a solid assumed to be comprised of cylindrical pores of uniform size. Petersen's results:

$$X = \frac{\epsilon_0}{1-\epsilon_0}\left[\xi^2\left(\frac{G-\xi}{G-1}\right) - 1\right] \tag{3}$$

and

$$S = S_0 \frac{\xi(2G - 3\xi)}{(2G-3)} \tag{4}$$

where

$$\frac{4}{27}\epsilon_0 G^3 - G + 1 = 0$$

relate the conversion and pore surface area to the instantaneous uniform pore radius. Initial pore intersections are modeled through a geometric assumption, and the treatment ignores any formation of a product layer. Calvelo and Cunningham (1970) have extended Petersen's model to include the formation of a solid product that has negligible diffusional resistance.

More recently, Bhatia and Perlmutter (1980, 1981a) and Gavalas (1980) have independently formulated a model that accounts for the random intersections of the pores in a solid with a pore-size distribution. For reactions with a solid product, Bhatia and Perlmutter (1981a) have derived the reaction rate

$$\frac{dX}{dt} = \frac{k_s S_0 C(1-X)\sqrt{1-\psi \ln(1-X)}}{(1-\epsilon_0)\left[1 + \frac{\beta Z}{\psi}\left[\sqrt{1-\psi\ln(1-X)} - 1\right]\right]} \tag{6}$$

where the parameter β characterizes the diffusional resistance to the flow of A in the layer of product Q assumed to be thin. Equation 6 can represent systems with a rate maximum as can also the model of Petersen (1957). The pore reaction model of Hashimoto and Silveston (1973), requiring several fitted parameters, does not allow for product formation, and the model of Ramachandran and Smith (1977b) neglects pore intersections, thereby predicting an ever-increasing reaction rate under conditions of kinetic control.

Each model must include some representation of the manner in which the product Q is formed and deposited. In the grain models, it is assumed that a shell of product is formed in each grain around an unreacted core of B. Thus, for the spherical grain model the radius of the grain is given by

$$r_g = r_{g0}[1 + (Z-1)]X^{1/3} \tag{7}$$

This implies that the grain size and the pore surface area increase monotonically with conversion for positive values of the volume ratio Z, even though the porosity decreases according to

$$\epsilon = \epsilon_0 - (Z-1)(1-\epsilon_0)X \tag{8}$$

Such an assumption ignores the loss in the surface exposed to the fluid A in the pores as the expanding grains begin to intersect at higher conversions. Thus, Eq. 2 which was derived by assuming that each grain is fully exposed to the fluid A can only be an approximation. For the random pore model, Eq. 6 embodies the assumption that the product layer is thin: the pore surface area is effectively the same as the reaction surface area.

In this paper, a generalized treatment of fluid-solid reactions is presented in terms of the movement of the internal reaction surfaces in the solid B, and the analysis is applied to the several models discussed above. To allow for intraparticle concentration gradients the usual representation (Smith, 1970), assuming equimolar counterdiffusion and the pseudosteady-state hypothesis (Bischoff, 1963; Luss, 1968) gives

$$\frac{1}{\eta^2}\frac{\partial}{\partial\eta}\left(D_e^* \eta^2 \frac{\partial C^*}{\partial \eta}\right) = \phi^2 \frac{dX}{d\tau} \tag{9}$$

with boundary conditions

$$\frac{\partial C^*}{\partial \eta} = 0 \text{ at } \eta = 0$$
$$\frac{\partial C^*}{\partial \eta} = \frac{Sh(1-C^*)}{D_e^*} \text{ at } \eta = 1 \tag{10}$$

for spherical particles. Following Satterfield (1970) and Smith (1970), the effective diffusivity varies with conversion according to

$$D_e^* = \frac{\epsilon^* \gamma(\epsilon_0)}{\gamma(\epsilon)} \tag{11}$$

MODEL DEVELOPMENT

As a porous solid undergoes an isothermal irreversible reaction, chemical change is initiated on the pore walls from which reaction surfaces progress inwards as conversion proceeds, leaving behind a layer of product Q through which the reactant fluid must diffuse. The pore surface for diffusive entry must be distinguished from the reaction surface at all times after the initial instant. As reaction proceeds each point on the reaction surface moves into the unreacted solid B at the instantaneous speed

$$\frac{dh_r}{dt} = k_s C_i \tag{12}$$

where h_r is the distance along the curve traced by any point on the reaction surface as it moves in the normal direction; C_i is the concentration of fluid A on the reaction interface. It should be emphasized that C_i is exactly uniform over the entire reaction surface only for a solid in which the surface curvature is everywhere uniform. Thus, for the grain model, this would require that all the grains have the same size, or for the random pore model, that the nonoverlapped pores have the same size. This assumption may also be used when such restrictions are not strictly satisfied, but then the concentration of fluid A is to be regarded as an effective or averaged value on the reaction surface.

Because the reaction product Q generally occupies a different volume than the stoichiometrically equivalent reactant B, the pore surface also moves in a direction assumed always normal to itself from its initial position at $h = 0$ to $h = h_p(X)$ at conversion X. The space between h_p and h_r is filled with reaction product Q. Figure 1 illustrates the motion of the pore and reaction surfaces separated by the product Q, in a single pore. In Figure 1(a) $Z > 1$, and h_p moves in the negative h direction; Figure 1(b) depicts $Z < 1$, the pore surface moving in the positive h direction. If it is assumed that

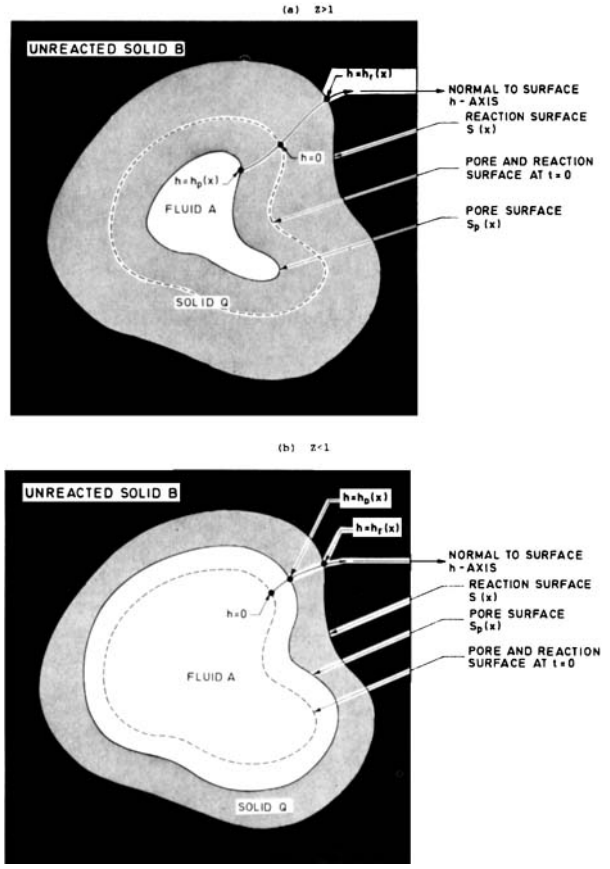

Figure 1. Development of pore and reaction surface in a single pore.

diffusion through the product occurs unidimensionally in the h direction, that is, that all points a distance h away from the original pore surface form contours of constant concentration, steady-state reactant conservation in the product layer gives

$$\frac{\partial}{\partial h}\left[S_d(h)\frac{\partial C_A}{\partial h}\right] = 0 \tag{13}$$

where $S_d(h)$ is the surface area of the contour formed by all points a distance h away from the original pore surface, measured along the normal direction. Since the reaction surface also moves in the normal direction, $S_d(h)$ must also represent the area of the reaction surface when it was at position h. If $Z > 1$ then the pore surface moves in the negative h direction. Thus:

$$S_d(h) = \begin{cases} S(h), & 0 \leq h \leq h_r \\ S_p(h), & h_p \leq h \leq 0 \end{cases} \tag{14}$$

The boundary condition for Eq. 13 at the pore surface is

$$C_A = C \text{ at } h = h_p \tag{15}$$

Equating the reaction and diffusion rates for fluid A at the reaction surface provides the other boundary condition

$$-D_p\left(\frac{\partial C_A}{\partial h}\right) = \frac{\rho a}{Mb}\left(\frac{dh_r}{dt}\right) \text{ at } h = h_r \tag{16}$$

Integrating Eq. 13 with the boundary conditions provides the concentration of fluid A at the reaction interface:

$$C_i = \frac{D_p C}{\left[D_p + \dfrac{\rho a k_s S(h_r)}{Mb}\displaystyle\int_{h_p}^{h_r}\frac{dh^*}{S_d(h^*)}\right]} \tag{17}$$

Expressing the local reaction rate in terms of the motion of this interface

$$\frac{dX}{dt} = \frac{S(h_r)}{(1-\epsilon_0)}\frac{dh_r}{dt} \tag{18}$$

and substituting Eqs. 12 and 17 yields

$$\frac{dX}{dt} = \frac{D_p k_s C S(h_r)}{(1-\epsilon_0)\left[D_p + \dfrac{k_s \rho a S(h_r)}{Mb}\displaystyle\int_{h_p(X)}^{h_r(X)}\frac{dh^*}{S_d(h^*)}\right]} \tag{19}$$

To each position h^* of the reaction surface or pore surface there corresponds a conversion X'. To reexpress the integrand of Eq. 19 in terms of this conversion, it is convenient to introduce the transformation

$$X^* = \frac{1}{(1-\epsilon_0)}\int_0^{h^*} S_d(h)dh, \quad h_p(X) \leq h^* \leq h_r(X) \tag{20}$$

It should be recognized that $|X^*|$ represents the volume of the product lying between $h = 0$ and $h = h^*$, per unit volume of the original solid phase. Therefore, the conversion corresponding to the position h^* of the reaction surface is

$$X' = X^*, \quad 0 < h^* \leq h_r(X) \tag{21}$$

similarly the conversion X' when the pore surface was at position h^* may be written as

$$X' = \frac{X^*}{(1-Z)} \tag{22}$$

over $h_p(X) \leq h^* \leq 0$ for $Z > 1$, and over the interval $0 \leq h^* \leq h_p(X)$ for $Z < 1$. Both h_p and X^* are negative for $Z > 1$. Equations 19 and 20 and the above arguments provide

$$\frac{dX}{d\tau} = \frac{S^*(X)C^*}{1 + \dfrac{\beta}{2}S^*(X)\displaystyle\int_{(1-z)X}^{X}\frac{dX^*}{S_d^{*2}(X^*)}} \tag{23}$$

and combination with Eqs. 14, 21 and 22 gives

$$\frac{dX}{d\tau} = \frac{S^*(X)C^*}{1 + \dfrac{\beta}{2}S^*(X)\left[\displaystyle\int_0^X\left[\frac{1}{S_{(X')}^{*2}} + \frac{Z-1}{S_p^{*2}(X')}\right]dX'\right]} \tag{24}$$

to express the instantaneous local reaction rate at any radial position in the particles of solid B. If these particles are considered spherical, Eqs. 8 to 11 may be used to introduce the associated transport effects, but if intraparticle and boundary layer diffusional resistances are negligible, $C^* = 1$ everywhere, and Eq. 24 may be rearranged and integrated to yield

$$\tau = \int_0^X \frac{dX_1}{S^*(X_1)} + \frac{\beta}{2}\int_0^X\int_0^{X_1}\left[\frac{1}{S^{*2}(X')} + \frac{Z-1}{S_p^{*2}(X')}\right]dX'dX_1 \tag{25}$$

In the event of reaction control, $\beta \to 0$, and the first term in the lefthand side of Eq. 25 dominates. This result could also have been deduced from Eqs. 12 and 18. When product layer diffusion dominates, $\beta \to \infty$, and the second term becomes more important.

To obtain specific solutions for $X(t)$ beyond the above discussion, it is necessary to provide models of the internal structure of the solid. Each such choice of model yields appropriate expressions $S^*(X)$ and $S_p^*(X)$ for substitution in the integrands of Eq. 24 or 25. To this end three different models of the solid structure are considered in the ensuing discussion: (1) the grain model (Szekely et al., 1976); (2) the Petersen (1957) model; and (3) the random pore model (Bhatia and Perlmutter, 1980; Gavalas, 1980).

Grain Model

If the solid is treated as being composed of equally-sized grains, the variation of the reaction surface with conversion follows:

$$S^*(X) = (1-X)^m \tag{26}$$

and for the pore surface

$$S_p^*(X) = [1 + (Z-1)X]^m \tag{27}$$

For spherical grains the shape factor $m = 2/3$. For cylindrical grains $m = 1/2$, and for flat plate grains $m = 0$. Any of these values

may be introduced into Eqs. 26 and 27 and combined with Eq. 24 to derive the expression for the reaction rate. As an example, for spherical grains, Eq. 24 becomes

$$\frac{dX}{d\tau} = \frac{(1-X)^{2/3}C^*}{1+\frac{\beta}{2}(1-X)^{2/3}\int_0^X\left[\frac{1}{(1-X')^{4/3}}+\frac{Z-1}{[1+(Z-1)X]^{4/3}}\right]dX'} \quad (28)$$

which integrates to the result in Eq. 2.

Petersen Model

The Petersen (1957) model which results in Eqs. 3 and 4 for a network of intersecting pores has hitherto been solved only for the case when there is no product layer diffusional resistance. The result provided by Petersen can be obtained by substituting Eqs. 3 and 4 into Eq. 24 with $\beta = 0$, and solving together with Eqs. 8 to 11. An analytic result for kinetic control in the absence of any significant intraparticle or external concentration gradients has also been provided (Szekely and Evans, 1976).

No solution has been derived for this model, however, in the presence of a product layer with a significant diffusional resistance. For this case, it is necessary to account for the deposition of this product layer in terms of the variation of the pore surface area with conversion, before eq. 24 can be solved. If it is assumed that the pore surface remains cylindrical and the intersection shapes are unchanged as the product layer is deposited, and further that the pore radii are uniform as reaction occurs, Eq. 4 remains valid in the presence of a product layer, with $\xi(X)$ replaced by $\xi_p(X)$, the pore radius at conversion X. Thus

$$S_p^*(X) = \xi_p(X)\left(\frac{2G-3\xi_p(X)}{2G-3}\right) \quad (29)$$

Similarly, Eq. 3 may be used to relate the uniform pore radius to the conversion, by substituting the fractional change in volume of the solid phase in placed of X, to give

$$\frac{\epsilon-\epsilon_0}{1-\epsilon_0} = \frac{\epsilon_0}{1-\epsilon_0}\left[\xi_p^2\left(\frac{G-\xi_p}{G-1}\right)-1\right] \quad (30)$$

which, upon combining with Eq. 8 yields

$$X = \frac{\epsilon_0}{(1-\epsilon_0)(Z-1)}\left[1-\frac{\xi_p^2(G-\xi_p)}{G-1}\right] \quad (31)$$

Equations 29 and 31 implicitly relate the total pore surface area to the conversion. Regardless of the product deposition Eqs. 3 and 4 relate the conversion and reaction surface area to the radius of the cylinders comprising the reaction surface. Substitution of Eqs. 3, 4, 29, and 31 into Eq. 24 results in

$$\frac{dX}{d\tau} = \frac{C^*}{\frac{1}{S^*(X)}+\frac{\epsilon_0(2G-3)^2\beta}{2(G-1)(1-\epsilon_0)}\left[\int_1^{\xi(X)}\frac{d\xi^*}{\xi^*(2G-3\xi^*)}-\int_1^{\xi_p(X)}\frac{d\xi_p^*}{\xi_p^*(2G-3\xi_p^*)}\right]} \quad (32)$$

which integrates to

$$\frac{dX}{d\tau} = \frac{C^*}{\frac{1}{S^*(X)}+\frac{\beta\epsilon_0(2G-3)^2}{4G(G-1)(1-\epsilon_0)}ln\left[\frac{\xi(2G-3\xi_p)}{\xi_p(2G-3\xi)}\right]} \quad (33)$$

Equation 33 may be combined with Eqs. 3, 4, 31 and 8 to 11 to obtain the conversion-time behaviour via a numerical procedure. If surface reaction and product layer diffusion dominate, $C^* = 1$ everywhere, and Eqs. 8 to 11 may be eliminated. In this case integration of Eq. 33 yields in combination with Eqs. 3, 4 and 31:

$$\tau = \frac{\epsilon_0}{(1-\epsilon_0)}\left(\frac{2G-3}{G-1}\right)(\xi-1) + \frac{\beta\epsilon_0^2(2G-3)^2}{4G(G-1)^2(1-\epsilon_0)^2}\left[F(\xi)+\frac{F(\xi_p)}{(Z-1)}\right] \quad (34)$$

where ξ and ξ_p are related to the instantaneous conversion through Eqs. 3 and 31, respectively, and

$$F(\xi) = \frac{4}{27}G^3\,ln\left(\frac{2G-3\xi}{2G-3}\right)+(G\xi^2-\xi^3)\,ln\left(\frac{\xi}{2G-3\xi}\right) + (G-1)\,ln\,(2G-3)-\frac{1}{3}G(\xi^2-1)+\frac{2}{9}G^2(\xi-1) \quad (35)$$

When $Z = 1$, $\xi_p = 1$ for all X, giving $F(\xi_p) = 0$. In such a case

$$\lim_{Z\to 1}\left[\frac{F(\xi_p)}{(Z-1)}\right] = [\xi^2(G-\xi)-(G-1)]\,ln\,(2G-3) \quad (36)$$

which combines with Eqs. 34 and 35 to provide the result for $Z = 1$:

$$\tau = \frac{\epsilon_0}{(1-\epsilon_0)}\left(\frac{2G-3}{G-1}\right)(\xi-1) + \frac{\beta\epsilon_0^2(2G-3)^2}{4G(G-1)^2(1-\epsilon_0)^2}H(\xi) \quad (37)$$

where

$$H(\xi) = \frac{4}{27}G^3\,ln\left(\frac{2G-3\xi}{2G-3}\right)+(G\xi^2-\xi^3)\,ln\left[\frac{\xi(2G-3)}{(2G-3\xi)}\right] - \frac{1}{3}G(\xi^2-1)+\frac{2}{9}G^2(\xi-1) \quad (38)$$

with ξ related to the instantaneous conversion through Eq. 3, and G related to ϵ_0 through Eq. 5.

Random Pore Model

The random pore model (Bhatia and Perlmutter, 1980, 1981a; Gavalas, 1980) considers the pores of the solid B to be comprised of a network of randomly overlapping cylinders from which a reaction surface grows. As a result of overlap, there is some loss in volume and surface area of the cylindrical system. Bhatia and Perlmutter (1980) have shown that if all the cylinders are growing at the same rate, the area of the reaction surface as it grows from the original pore surface is given by

$$S^* = \left(\frac{1-V}{1-\epsilon_0}\right)\sqrt{1-\psi\,ln\,\frac{1-V}{(1-\epsilon_0)}} \quad (39)$$

The restriction that all the cylinders grow at the same rate is rigorously true in the absence of a product layer diffusional resistance, or when all the nonoverlapped cylinders have the same size; however, Eq. 39 also may be used for thin product layers for which the curvature of the reaction surface has little influence. The thin layer result should probably hold to about 60% conversion, as for the Jander (1927) solution to the shrinking core problem.

In the present work where a network comprised of uniformly-sized nonoverlapped cylinders is considered, Eq. 39 will hold rigorously at all levels of conversion. Rewritten in terms of the conversion Eq. 39 is:

$$S^*(X) = (1-X)\sqrt{1-\psi\,ln\,(1-X)} \quad (40)$$

Since the pore surface is assumed to move in the normal direction, its evolution can also be considered to be the motion of the surface of a set of overlapping cylinders. For uniform-size cylinders, Eq. 39 is valid for the pore surface area, but with V replaced by the porosity ϵ. Combining this observation with Eqs. 8 and 39 provides

$$S_p^*(X) = [1+(Z-1)X]\sqrt{1-\psi\,ln\,[1+(Z-1)X]} \quad (41)$$

The local reaction rate of any conversion can be found by substitution of Eqs. 40 and 41 into Eq. 24, and rearrangement:

$$\frac{dX}{d\tau} = \frac{(1-X)\sqrt{1-\psi\,ln\,(1-X)}C^*}{1+\frac{\beta}{2}(1-X)\sqrt{1-\psi\,ln\,(1-X)}\int_{(1-z)X}^{X}\frac{dX'}{(1-X')^2[1-\psi\,ln\,(1-X')]}} \tag{42}$$

Since it has been assumed that all the nonoverlapped cylinders have a uniform radius, the results derived by Bhatia and Perlmutter (1980, 1981b) reduce to

$$\psi = \frac{4\pi L_{E0}}{S_{E0}^2} \tag{43}$$

and

$$\psi = \frac{1}{V_{E0}} = \frac{1}{ln\left(\frac{1}{1-\epsilon_0}\right)} \tag{44}$$

By combining Eq. 44 with Eqs. 8 and 41, it is found that $S_p^* \to 0$ as $\epsilon \to 0$, consistent with expectation. The same observation may also be confirmed for the results obtained from the Petersen model by using Eq. 8, 29 and 31 developed above.

NUMERICAL RESULTS

Conversion vs. Time

To compare and contrast the various models, solutions were computed to Eqs. 2 for the grain model, Eqs. 3, 37 and 38 for the Petersen model, and Eq. 42 for the random pore model, for the case when intraparticle and boundary layer concentration gradients are negligible. To solve Eq. 42, the transformation

$$Y = \int_{(1-z)X}^{X}\frac{dX'}{(1-X')^2[1-\psi\,ln\,(1-X')]} \tag{45}$$

was introduced, so that

$$\frac{dY}{dX} = \frac{1}{(1-X)^2[1-\psi\,ln\,(1-X)]} + \frac{(Z-1)}{[1+(Z-1)X]^2[1-\psi\,ln\,(1+(Z-1)X]} \tag{46}$$

and

$$\frac{dX}{d\tau} = \frac{C^*(1-X)\sqrt{1-\psi\,ln\,(1-X)}}{1+\frac{\beta}{2}(1-X)Y\sqrt{1-\psi\,ln\,(1-X)}} \tag{47}$$

with initial condition $X = Y = 0$ at $\tau = 0$. Equations 46 and 47 were solved numerically using a Runge-Kutta-Merson technique. Solutions were also obtained from an integration of Eq. 6, the thin layer result for the random pore model. As seen in Figure 2, the random pore model agrees remarkably well with the spherical grain model at all levels of β for $\psi = 1$ and $Z = 1$. The simpler thin layer result for the random pore model also agrees with these two up to about 60% conversion, deviating at higher conversions because of the assumption that the concentration gradient of A in the product layer is linear. The results from the Petersen model, however, differ significantly from those of the other models at all levels of β except at low conversions below about 40%.

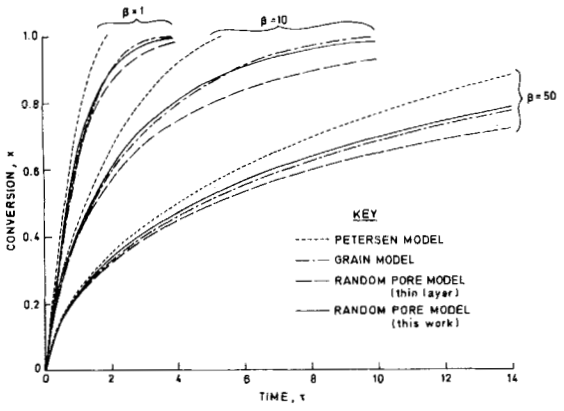

Figure 2. Comparison of Conversion predictions for several models for various values of β. Parameters are: $\psi = Z = 1$, $\phi = 0$.

Surface vs. Conversion

To further examine the differences among the various models, it is instructive to compare the predictions regarding the growth of the pore surfaces and reaction surfaces with conversion. Figure 3 shows the pore surfaces obtained from Eq. 27 for the grain model, Eqs. 29 and 31 for the Petersen model, and Eq. 41 for the random pore model, for various values of the parameter Z. The pore surfaces for Z = 0, which also correspond to the reaction surfaces at all levels of Z, are in good agreement for the grain model and the random pore model; however, the Petersen result shows a larger reaction surface at all conversions, consistent with the more rapid conversion, Figure 2.

For Z = 1 all the models are in agreement since the pore surface is assumed unchanged. At values of $Z > 1$, however, even the grain and random pore models are in disagreement, the former predicting a monotonically increasing pore surface, and the latter showing a decrease in the surface after some conversion. It would seem that this random pore result is more realistic, since for Z large enough that Eq. 8 predicts pore closure prior to complete conversion, the model is consistent in leading to $S_p^* \to 0$ with increasing conversion. The Petersen model predicts a lower pore surface than either the grain or random pore models at values of Z higher than unity, although it does show a decrease in the pore surface after some conversion.

It is worthy of note that there are relatively large differences in the pore surfaces between the grain and random pore models for

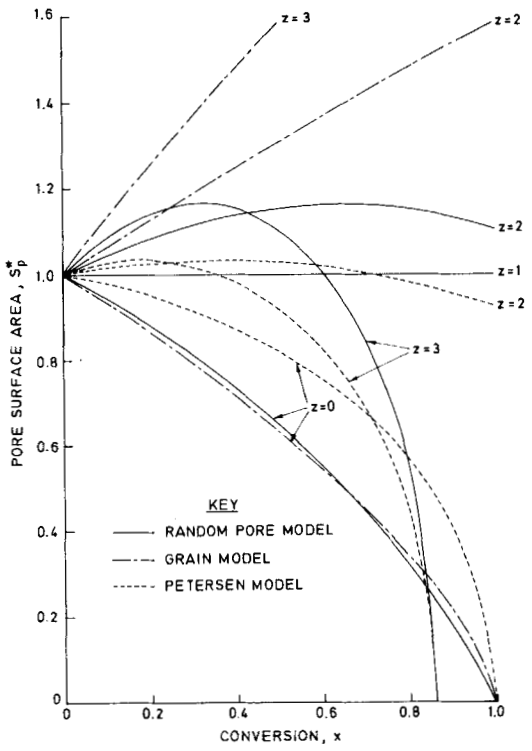

Figure 3. Predicted development of the pore surface compared for various models.

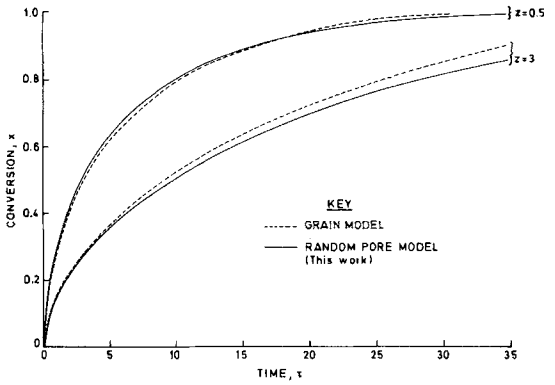

Figure 4. Comparison of Conversions predicted by random pore and grain models. Parameters are: $\psi = 1$, $\beta = 50$, $\phi = 0$.

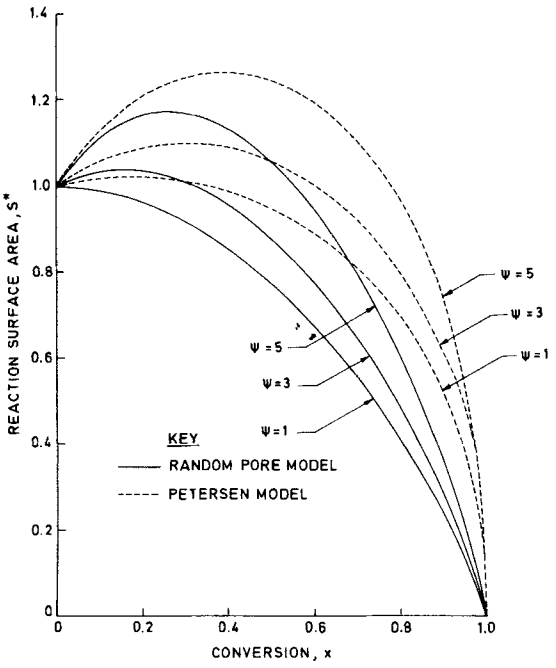

Figure 5. Effect of ψ on the development of the reaction surface, compared for random pore and Petersen models.

$Z > 1$, but only small differences in the predicted conversions, Figure 4. Evidently, the conversion-time predictions are more strongly affected by differences in the reaction surface than of the pore surface. Thus, the grain and random pore models, which show similar behavior of the reaction surface, are in agreement, as to conversion, while the Petersen model is not (c.f. Figure 2). This argument is further strengthened by the results shown in Figure 5 which compares the reaction surfaces for the random pore and Petersen models, computed using Eqs. 3, 4, and 40, with ϵ_0 given by Eq. 44. The deviations are considerable even for low porosities, in agreement with the divergent predictions of the two models shown in Figure 2. Under conditions of kinetic control, conversion-time measurements alone suffice to distinguish between these models.

A further comparison of predicted pore surfaces for the random pore and Petersen models is provided in Figure 6 which shows the effect of ψ when $Z = 2$. The void fraction ϵ_0 is related to ψ through Eq. 44. The models are in very good agreement for values of $\psi > 2$ and hence $\epsilon_0 < 0.4$, but at higher porosities the Petersen model predicts lower pore surfaces. By differentiating Eq. 41, it may be shown that the maximum in the pore surface for the random pore model occurs at the conversion

$$X_M = \frac{1}{(Z-1)}\left[e^{(1/\psi - 1/2)} - 1\right] \tag{48}$$

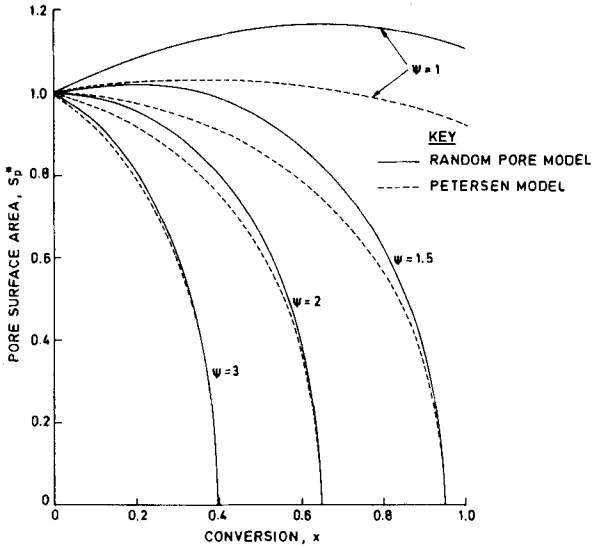

Figure 6. Effect of ψ on the development of the pore surface, compared for random pore and Petersen models.

Equation 48 combined with Eq. 44 gives the limiting value Z for which a maximum can occur:

$$Z_M = e^{-1/2}e^{1/\psi} = \frac{e^{-1/2}}{(1-\epsilon_0)} \tag{49}$$

For $\psi > 2$, the pore surface increases monotonically for $Z_m \leq Z < 1$ and decreases for $Z > 1$. Thus, for $\psi > 2$, a maximum in the pore surface area exists only for $Z < Z_m$. Similarly for $\psi < 2$ a maximum exists only for $Z > Z_m$, the pore surface monotonically increasing if $1 < Z \leq Z_M$, and decreasing if $Z < 1$. Equation 49 predicts for example that a maximum occurs in Figure 3 only for $Z > 1.65$. Similarly for the Petersen model, the position of the maximum pore surface is obtained using Eqs. 29 and 31 as

$$X'_M = \frac{2\epsilon_0 - 1}{2(1-\epsilon_0)(Z-1)} \tag{50}$$

with the limiting value of Z for which a maximum exists in the pore surface area given by

$$Z'_M = \frac{1}{2(1-\epsilon_0)} \tag{51}$$

Thus, for $\epsilon_0 < 0.5$ a maximum occurs for $Z < Z'_M$ while for $\epsilon_0 > 0.5$ a maximum occurs for $Z < Z'_M$.

Maximum Conversion

Certain fluid solid reactions are characterized by incomplete conversion obtained as a result of premature pore closure at the surface of reacting particles (Hartman and Coughlin, 1970; Georgakis et al., 1979; Bhatia and Perlmutter, 1981a,b). This only occurs for reaction systems for which $Z > 1$; i.e., for small enough ϵ_0, Eq. 8 predicts that $\epsilon = 0$ at some conversion less than unity. For such reactions, it may be anticipated that pore closure occurs first at the surface where reaction is most rapid, and that when the surface porosity is zero reaction ceases, since no further penetration of A into the particle can occur. For the reaction between lime and SO_2, for example, the experimental maximum conversions can be anticipated by either the grain or the random pore models (Hartman and Coughlin, 1976; Bhatia and Perlmutter, 1981b).

To compare the predictions of the maximum conversion developed here with those of the thin product layer approximation of the random pore model, Eqs. 8 to 11 were solved together with the rate Eqs. 46 and 47 of the new model, and then also with Eq. 6 of the earlier thin layer analysis, assuming that tortuosity is constant (i.e., $D_e^* = \epsilon^*$) with parameter values chosen to be in the range of those studied by Hartman and Coughlin (1976). Details of the numerical procedure are provided by Bhatia (1981). Figure

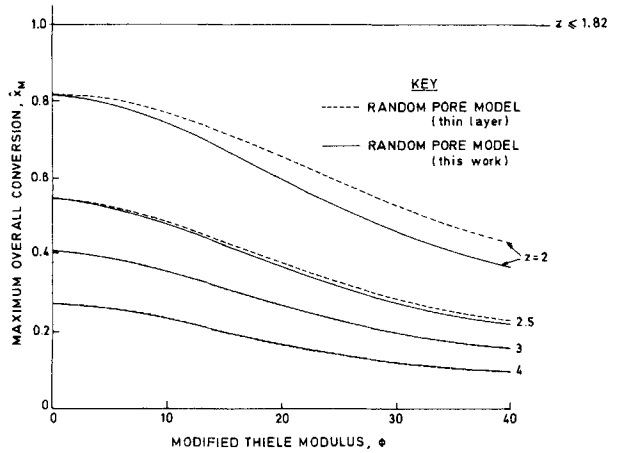

Figure 7. Effect of Thiele modulus on maximum conversion. Parameters are: $\epsilon_0 = 0.45$, $\beta = 150$.

TABLE 1. MODEL PARAMETERS APPLIED TO DATA OF BORGWARDT (1970)

$a = b = 1$
C_b = calculated at each temperature for 3,000 ppm SO_2 (dry basis)
$Sh = \infty$
$\alpha_l = 16.9 \times 10^{-3}$ m^3/kmol
$\alpha_s = 52.2 \times 10^{-3}$ m^3/kmol
$\omega_0 = 0.54$
$\rho_b = 1.59 \times 10^3$ kg/m^3
$R_o = 48\ \mu$m
$\epsilon_0 = 0.56$
$S_0 = 5.9 \times 10^6$ m^2/m^3
$\psi = 1.2$

TABLE 2. RATE PARAMETERS ESTIMATED FROM DATA OF BORGWARDT (1970)

Temp. K	$k_s \times 10^5$ (m^4/kmol·s)	β	$D_p \times 10^{12}$ (m^2/s)
923	1.2	50	1.25
1,033	2.55	22.5	5.9
1,143	4.74	14.7	16.7
1,253	8.34	8.5	51

7 reveals that there is very little difference in the maximum conversions predicted by the two models. As anticipated from the lower conversion in the interior at the time of surface pore closure, the maximum conversion decreases with increase in the intraparticle diffusional resistance represented by the modified Thiele modulus. For $\epsilon_0 = 0.45$, Eq. 8 predicts that complete conversion occurs for $Z \leq 1.82$. For larger values of Z incomplete conversions are found, and the deviations between the two models are greater at the low values of Z, where surface pore closure occurs at higher levels of local conversion. The thin layer approximation is less accurate above about 60% conversion.

APPLICATION TO EXPERIMENTAL DATA

As an illustration of its use, the new model was applied to the data of Borgwardt (1970) on the SO_2-lime reaction. These data serve as a useful medium of comparison, since they were previously analyzed (Bhatia and Perlmutter, 1981a, 1981b) by using the thin layer approximation to the random pore model. The parameter levels used for computation are repeated in Table 1 for reference. The model Eq. 42 was solved simultaneously with Eqs. 8 to 11, the effective intraparticle diffusivity and the factor Z being calculated through Eqs. 16 to 20 and 22, 23 of the earlier work. The rate constants had previously been calculated from the initial rates, Table 2.

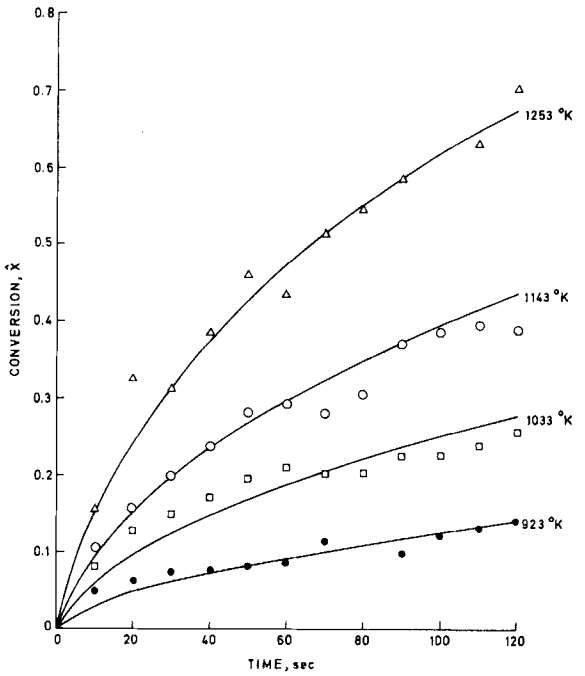

Figure 8. Application of random pore model to data of Borgwardt (1970); solid lines represent model calculations.

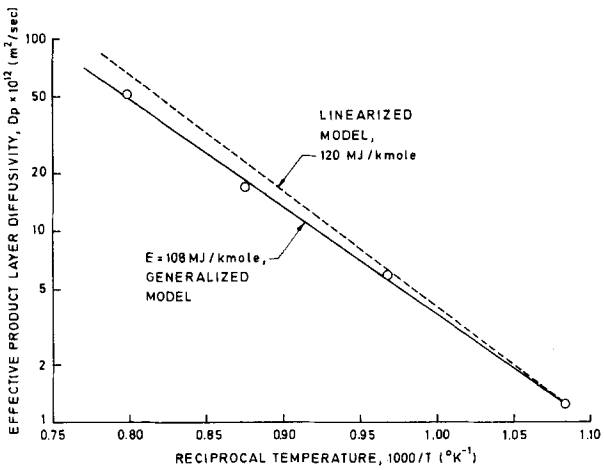

Figure 9. Arrhenius plot for product layer diffusivity.

The model predictions, Figure 8, were fitted to the data of Borgwardt by varying only the effective product layer diffusivity at each temperature. The estimated best-fit values of this parameter are given in Table 2, from which the activation energy is 108 MJ/kmol, Figure 9. For comparison, the results obtained via the linearized model are superimposed on the same figure, demonstrating the somewhat higher activation energy of 120 MJ/kmol. The fit of the new model yields relatively smaller values of the effective product layer diffusivity as temperature increases, consistent with the slower reaction rates predicted by the linearized analysis (c.f. Figure 2). This difference is more marked at the higher temperatures where the data of Borgwardt (1970) show substantially enhanced conversions (c.f. Figure 8).

DISCUSSION

In representing the development of the pore surfaces for the random pore and Petersen cases, it has been assumed here that they are comprised of intersecting cylinders, neglecting as insignificant any rounding off that may occur at points of overlap as the product layer is deposited. A second assumption that warrants somewhat

further discussion is that diffusion of fluid A in the product layer occurs unidimensionally in the normal direction. Such an assumption is exact for several solid structures with regular geometries. Thus, in the grain model, product layer diffusion occurs radially inward in each grain.

Similarly, in a solid comprised of nonoverlapped cylindrical pores (Ramachandran and Smith, 1977), diffusion would also occur radially inward into the product layer coating the pores. This assumption can also be a close approximation for other geometries even when not exactly rigorous. For initially cubical grains, for example, if the product is deposited as a cubical annulus, the iso-concentration surfaces are not cubical as fluid A diffuses through the annulus. Nevertheless, one may with little error consider the iso-concentration surfaces to be cubical in calculating the flux of fluid A through the product layer. Similarly in a product layer deposited in a structure comprising a network of randomly overlapping cylinders (e.g., the Petersen or the random pore models), irregularities are created at points of intersection and diffusion at these points may not be radially inward.

However, a tractable solution to the problem is obtained by assuming that diffusion occurs in the normal direction and allowing for the change in the diffusion surface in this direction. It should be noted here that if the intersection-produced changes in the diffusion surface are not accounted for one arrives at the result of Ramachandran and Smith (1977b) for the concentration of fluid A at the reaction interface:

$$C_i = \frac{D_p C}{D_p + \dfrac{\rho a k_s r_{p0} \xi}{Mb} \ln\left(\dfrac{\xi}{\xi_p}\right)} \tag{52}$$

The difference between this result and that obtained by combining Eq. 17 with the appropriate surface area expressions derived in this paper for the Petersen or the random pore models is due precisely to the effect of intersections.

ACKNOWLEDGMENT

This research was supported by NSF Grant No. CPE-8000291.

NOTATION

a,b = stoichiometric coefficients
C = local concentration of fluid A in particle
C_A = local concentration of fluid A in product layer
C_b = bulk concentration of fluid A
C_i = concentration of A at the reaction surface
C^* = C/C_b
D_e = effective diffusivity of fluid A in particle
D_{e0} = initial value of D_e
D_e^* = D_e/D_{e0}
D_p = effective diffusivity of fluid A in product layer
h = position in product layer, measured from initial pore surface
$h_p(X)$ = position of pore surface at conversion X
$h_r(X)$ = position of reaction surface at conversion X
k_m = boundary layer mass transfer coefficient
k_s = rate constant for surface reaction
L_{E0} = total length of nonoverlapped system per unit volume, at $t = 0$
m = grain shape factor, or reaction order with respect to solid B
M = molecular weight of solid B
p, q = stoichiometric coefficients
r_g = grain radius
r_{g0} = r_g at $t = 0$
r = radius of cylinder comprising the reaction surface in Petersen model
r_p = cylindrical pore radius in Petersen model
r_{p0} = r_p at $t = 0$
R = radial position
R_o = particle radius
S = reaction surface are per unit volume
S^* = S/S_0
S_d = area of diffusion surface
S_{E0} = initial surface area of nonoverlapped system
S_p = pore surface area
S_p^* = S_p/S_0
S_0 = S at $t = 0$
Sh = $k_m R_o/D_{eo}$, modified Sherwood Number
t = time
V = volume enclosed by reaction surface, per unit volume of space
V_{E0} = initial volume of nonoverlapped system
X = local conversion
X_M, X_M' = position of maximum conversion
Y = transformation defined in Eq. 47
Z = ratio of volume of solid phase after reaction to that before reaction
Z_M, Z_M' = limiting value of Z

Greek Letters

β = $2k_s a\rho(1-\epsilon_0)/MbD_P S_0$
ξ = r/r_{p0}
ξ_p = $r_{p/r_{p0}}$
ϵ = porosity
ϵ_0 = ϵ at $t = 0$
ϵ^* = ϵ/ϵ_0
$\gamma(\epsilon)$ = tortuosity
η = R/R_o
ϕ = $R_o\sqrt{k_s a\rho S_0/MbD_{e0}}$, modified Thiele modulus
ψ = $4\pi L_{E0}/S_{E0}$, structural parameter
ρ = mass of solid per unit volume in original solid phase
τ = $k_s C_b S_0 t/(1-\epsilon_0)$, dimensionless time

LITERATURE CITED

Barner, H. E., and C. L. Mantell, "Kinetics of Hydrogen Reduction of Manganese Dioxide," *Ind. Eng. Chem. Process Design Develop.*, **7**, 285 (1968).

Bhatia, S. K., "The Effect of Pore Structure on the Kinetics of Fluid Solid Reactions," Ph.D. Thesis, University of Pennsylvania (1981).

Bhatia, S. K., and D. D. Perlmutter, "A Random Pore Model for Fluid-Solid Reactions: I. Isothermal, Kinetic Control," *AIChE J.*, **26**, 379 (1980).

Bhatia, S. K., and D. D. Perlmutter, "A Random Pore Model for Fluid-Solid Reactions: II. Diffusion and Transport Effects," *AIChE J.*, **27**, 247 (1981a).]

Bhatia, S. K., and D. D. Perlmutter, "The Effect of Pore Structure on Fluid-Solid Reactions: Application to the SO_2-Lime Reaction," *AIChE J.*, **27**, 226 (1981b).

Bischoff, K. B., "Accuracy of the Pseudo Steady State Approximation for Moving Boundary Diffusion Problems," *Chem. Eng. Sci.*, **18**, 711 (1963).

Borgwardt, R. H., "Kinetics of the Reaction of SO_2 with Calcined Limestone," *Environ. Sci. Technol.*, **4**, 59 (1970).

Calvelo, A., and R. E. Cunningham, "Kinetics of Gas-Solid Reactions," *J. Catalysis*, **17**, 1 (1970).

Calvelo, A. and J. M. Smith, "Intrapellet Transport in Gas-Solid Non-Catalytic Reactions," *Proceedings of Chemeca*, **70**, Paper 3.1, Butterworths, Australia (1971).

Gavalas, G. R., "A Random Capillary Model with Application to Char Gasification at Chemically Controlled Rates," *AIChE J.*, **26**, 577 (1980).

Georgakis, C., D. W. Chang, and J. Szekely, "A Changing Grain Size Model for Gas-Solid Reactions," *Chem. Eng. Sci.*, **34**, 1072 (1979).

Hartman, M., and R. W. Coughlin, "Reaction of Sulfur Dioxide with Limestone and the Grain Model," *AIChE J.*, **22**, 490 (1976).

Hashimoto, K., and P. L. Silveston, "Gasification: Part I. Isothermal Kinetic Control Model for a Solid with a Pore Size Distribution," *AIChE J.*, **19**, 259 (1973).

Jander, W., "Reaktionen im festen Zustande bei hoheren Temperaturen," *Z. Anorg. Allgem. Chem.*, **163**, 1 (1927).
Luss, D., "On the Pseudo Steady State Approximation for Gas Solid Reactions," *Can. J. Chem. Eng.*, **46**, 154 (1968).
Petersen, E. E., "Reaction of Porous Solids," *AIChE J.*, **3**, 442 (1957).
Ramachandran, P. A., and J. M. Smith, "Effect of Sintering and Porosity Changes on Rates of Gas-Solid Reactions," *Chem. Eng. J.*, **14**, 137 (1977a).
Ramachandran, P. A., and J. M. Smith, "A Single-Pore Model for Gas-Solid Non-Catalytic Reactions," *AIChE J.*, **23**, 353 (1977b).
Satterfield, C. N., *Mass Transfer in Heterogeneous Catalysis*, M.I.T. Press, Cambridge, MA (1970).
Smith, J. M., *Chemical Engineering Kinetics*, McGraw Hill, New York (1970).
Szekely, J., and J. W. Evans, "A Structural Model for Gas-Solid Reactions with a Moving Boundary," *Chem. Eng. Sci.*, **25**, 1091 (1970).
Szekely, J., J. W. Evans, and H. Y. Sohn, *Gas-Solid Reactions*, Academic Press, London (1976).

Manuscript received October 23, 1981; revision received April 12, and accepted April 26, 1982.

Discrete Cell Model of Pore-Mouth Poisoning of Fixed-Bed Reactors

Catalyst deactivation in an isothermal fixed-bed reactor under pore-mouth poisoning conditions is investigated theoretically using a discrete mixing cell model. Two fundamental relationships which characterize the poisoning process in the reactor are identified and incorporated into the model to develop a simple graphical procedure for a quick, general insight into the problem. This graphical method is extended to design pellet impregnation profiles along the reactor which would give nondeteriorating reactor performance up to a given time. The effects of various system parameters on the lifetime and conversion performance of the reactor are also examined analytically, graphically and numerically.

B. K. CHO and L. L. HEGEDUS

General Motors Research Laboratories
Warren, MI 48090
and
RUTHERFORD ARIS
University of Minnesota
Minneapolis, MN 55455

SCOPE

Deactivation of catalyst pellets due to pore-mouth poisoning and the associated performance degradation of fixed-bed catalytic reactors have been extensively treated by numerous investigators for the past two decades. However, all previous approaches were confined to continuum models in which the poisoning process is described by coupled partial differential equations.

The main purpose of this work is to investigate the poison accumulation and deactivation process in a fixed-bed catalytic reactor under pore-mouth poisoning conditions through the use of a discrete mixing cell model.

It is demonstrated that a useful insight into the reactor behavior can be readily obtained without solving the partial differential equations inherent to the continuum model, and furthermore the discrete model equations can be solved through a simple graphical procedure which plays a role similar to the McCabe-Thiele method in distillation column design. This graphical procedure is then employed to the optimum design of a poison-resistant catalytic reactor.

The effect of gas-phase dispersion on the reactor's lifetime is examined for various types of noble metal impregnation patterns in the catalyst pellets. The effects of noble metal loadings, the impregnation pattern, and the effective diffusivity of catalyst pellets as well as the effect of gas-phase mixing on the conversion performance of the reactor are studied.

CONCLUSIONS AND SIGNIFICANCE

The discrete mixing cell model developed in this paper demonstrates a clear computational advantage over the traditional continuum model for simulating the pore-mouth poisoning process in a fixed-bed catalytic reactor.

Due to its discrete nature, this model allows one to determine the poison profile, the lifetime, and the conversion performance of a fixed-bed reactor through a simple graphical procedure. This graphical procedure can be readily extended to investigate the optimum noble metal impregnation profiles along the reactor which would give non-deteriorating reactor performance throughout a given reactor operating time.

Mixing characteristics in the gas phase do not influence the reactor lifetime when catalyst pellets are uniformly or core impregnated. For subsurface or peripherally impregnated catalysts, however, the reactor lifetime becomes shorter with increased mixing in the gas phase.

For a first-order main reaction under pore-mouth poisoning, a plug-flow reactor gives higher conversion than a well-mixed reactor for shorter reactor operating times, while a well-mixed reactor gives higher conversion for longer operating times. There is a point in time when the two reactors give equivalent conversion performance.

INTRODUCTION

When a fixed-bed catalytic reactor operates under the condition that the reaction rate of the poison precursor (e.g., impurity in the feed) with the catalyst support or the catalytic sites is much faster than the poison precursor's diffusion rate through the pores, the overall poisoning process is limited by the rate of poison precursor diffusion across the poisoned shell of the catalyst. A quantitative understanding of such pore-mouth poisoning is of considerable

L. L. Hegedus is presently with W. R. Grace & Co., Columbia, MD 21044.